Invited Feature Article

NANOMATERIALS AND NANOTECHNOLOGY

Nanomaterials and Nanotechnology
Volume 8: 1–7

DOI: 10.1177/1847980418772402
journals.sagepub.com/home/nax
SAGE

Plasmonic nanospherical dimers for color pixels

Salma Alrasheed and Enzo Di Fabrizio

Abstract

Display technologies are evolving more toward higher resolution and miniaturization. Plasmonic color pixels can offer solutions to realize such technologies due to their sharp resonances and selective scattering and absorption at particular wavelengths. Metal nanosphere dimers are capable of supporting plasmon resonances that can be tuned to span the entire visible spectrum. In this article, we demonstrate numerically bright color pixels that are highly polarized and broadly tuned using periodic arrays of metal nanosphere dimers on a glass substrate. We show that it is possible to obtain RGB pixels in the reflection mode. The longitudinal plasmon resonance of nanosphere dimers along the axis of the dimer is the main contributor to the color of the pixel, while far-field diffractive coupling further enhances and tunes the plasmon resonance. The computational method used is the finite-difference time-domain method. The advantages of this approach include simplicity of the design, bright coloration, and highly polarized function. In addition, we show that it is possible to obtain different colors by varying the angle of incidence, the periodicity, the size of the dimer, the gap, and the substrate thickness.

Keywords

Color pixels, metamaterials, subwavelength optics, metasurfaces, plasmonics, display technology, displays, nanoparticles, nanophotonics

Date received: 24 October 2017; accepted: 19 March 2018

Topic: Nanophotonics
Topic Editor: Paola Prete

Introduction

Metal nanoparticles support collective electron oscillations known as surface plasmons. Such oscillations result in the localization of the fields beyond the diffraction limit and to its enhancement relative to the incident fields. This is in addition to the strong scattering and absorption of light at the resonance wavelength of the metal nanoparticle. These features are used in many devices including biosensors, solar cells, light-emitting devices, waveguides, and high-resolution imaging.[1–4] Among such applications are display technologies, which are evolving more toward higher resolution and miniaturization. Plasmonic color pixels can offer solutions to realize such technologies due to their sharp resonances and selective scattering and absorption at particular wavelengths and due to their size, allowing it to perform at resolutions beyond the diffraction limit. Examples of plasmonic color-generation devices include color filters,[5–15] high-resolution color pixels,[16–21] plasmonics combined with liquid crystals,[22] image printing beyond the diffraction limit,[23–26] transparent display,[27] and color holograms.[28–30] In this article, we demonstrate bright color pixels that are broadly tuned and highly polarized using periodic arrays of different metal nanosphere dimers on a glass substrate. Far-field diffractive coupling further enhances and tunes the resonance, narrowing its linewidth, which results in purer colors. The computational method used is the finite-difference time-domain method (FDTD) using the commercial software FDTD Lumerical Solutions v8.9.

PSE and BESE Divisions, King Abdullah University of Science and Technology, Thuwal, Kingdom of Saudi Arabia

Corresponding author:
Salma Alrasheed, PSE and BESE Divisions, King Abdullah University of Science and Technology, Thuwal 23955-6900, Kingdom of Saudi Arabia.
Email: salma.alrasheed@kaust.edu.sa

Display technologies including plasma displays, liquid crystal displays, and light-emitting diode displays use different color-producing media to produce color pixels such as the standard RGB color scheme pixel made up of the primary colors (blue, green, and red) under the illumination of a light source or through utilizing an electric voltage. These technologies are evolving toward more flexible displays, higher resolution, and higher energy efficiency.[16,26,27] Plasmonic color pixels offer the advantage of increased resolution and a wide range of color tunability by changing the dimensions or the geometry of the structure, the surrounding environment index, the polarization, or the angle of incidence of the exciting light. In addition, the ultrathin thickness of the structure supporting the plasmonic elements makes it suitable for integration in miniaturized devices. The periodicity is also comparable to the wavelength, which makes it possible to produce pixels that are smaller than conventional methods. Further, because plasmonic resonators are made of metals, they are more stable than chemical pigments and can endure higher temperatures and ultraviolet radiation.[5,10,11]

In this article, we show that periodic arrays of different metal nanosphere dimers on a glass substrate can produce bright color pixels that are broadly tuned and highly polarized. This is based on the fact that plasmonic nanoparticles show resonant selective scattering at particular wavelengths, while being almost transparent to other wavelengths. To produce the color pixels, nanosphere dimers made of aluminum (Al), silver (Ag), and gold (Au) are used for the blue, green, and red pixels, respectively. Al and Ag are more suitable than Au for shorter wavelengths, as Au nanoparticle resonances below 520 nm are quenched due to interband transitions.[16] In the case of the nanospherical dimer, we found that the longitudinal plasmon resonance along the axis of the dimer is the main contributor to the resonance and, therefore, to the color of the pixel. Far-field diffractive coupling enhances the scattering intensity and reduces the plasmon linewidth of the array.[31–38] Note that the glass substrate has the effect of redshifting the resonance and making the far-field diffractive coupling less efficient due to the inhomogeneous environment around the dimers.[39–43] However, it was shown that for large particles, diffractive coupling could still occur.[36,43,44] In addition, the glass substrate can result in additional peaks appearing at the blue side of the original resonance.[45–47] For appropriate periodicities, additional resonances can be suppressed to produce purer colors pixels. The advantage of using a dimer instead of a monomer is that it is polarization sensitive, which is consistent with display technologies, and it has the ability to enhance the far-field scattering intensity as the gap gets smaller.[48] Although it is hard to fabricate dimers relative to monomers, recent improvements in the fabrication techniques have been made.[49,50]

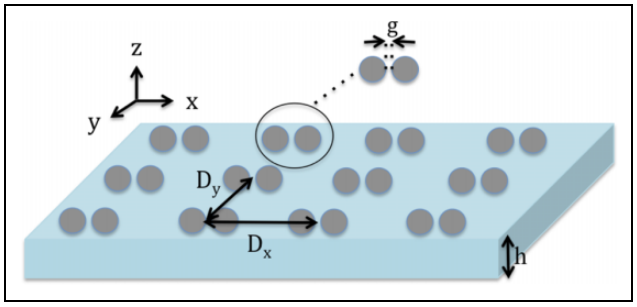

Figure 1. Schematic diagram of the plasmonic color pixel array of periodic metal nanosphere dimers on a glass substrate of thickness *h*. Polarized white light interacts with the dimers and selectively scatters back certain wavelengths. The gap distance between the spheres is *g* and the periodicity in *x* and *y* is D_x and D_y, respectively.

Structure and design

For the numerical optimization of the design, we tune the color of each pixel by changing the material and diameters of spheres, while keeping the gap fixed. This small gap also allows for a higher far-field scattering intensity[48] (see Online Supplementary Figure S1). In addition, we use far-field diffractive coupling to further enhance, tune, and narrow the plasmon linewidth by changing the periodicities of the array, D_x, and D_y, (dimer center to center distance in the x and y directions, respectively). The advantages of this approach include simplicity of the design, bright coloration, and highly polarized function. In addition, we show that it is possible to obtain different colors by varying the angle of incidence. Our design can also be used for transparent displays by projecting monochromatic light at the resonance wavelength. A schematic diagram of the array is shown in Figure 1.We use FDTD commercial software Lumerical to perform the numerical optimizations and calculate the reflection spectra. We use p-polarized white light (400–750 nm) to excite the arrays at normal incidence. This results in the excitation of the longitudinal plasmon resonance along the axis of the dimer, which is the main contributor resonance that produces the color of the pixel. This makes the array polarization selective that is compatible with display technologies. Each pixel consists of an array of identical nanosphere dimers with the same edge-to-edge spacing. We also numerically calculate the scattering and absorption cross-section efficiencies for the individual dimers to show diffractive coupling effects on the spectral peaks and linshapes.

In general, as the length of the dimer increases, its resonance redshifts; however, this is accompanied by a broader resonance due to an increase in radiative damping. This effect can be minimized using diffractive coupling to

Table 1. Parameters used for the RGB pixel arrays.

Color	Material	Array's resonance reflection peak wavelength (nm)	Sphere radius (nm)	D_x (nm)	D_y (nm)
Blue	Al	453	35	160	335
Green	Ag	520	40	245	360
Red	Au	637	50	380	480

RGB: Al: aluminum; Ag: silver; Au: gold.

achieve strong higher intensity and narrower peaks suitable for color displays. We choose D_x in all of the three arrays to be much smaller than the wavelength used, while D_y is varied to tune the resonance. This is because for a rectangular array, as our case, the periodicity perpendicular to the polarization vector is more important in determining the spectral shift and width of the resonance than the periodicity that is parallel to the polarization vector.[34] We designed RGB pixels in the reflection mode with their spectral peak positions corresponding to the wavelengths of blue (453 nm), green (520 nm), and red (637 nm). Table 1 lists the parameters used for each pixel array. The thickness of the glass substrate is 140 nm for all of the arrays. The gap size between the spheres is 3 nm for all of the dimers used. The complex refractive index for Ag, Al, and silicon dioxide is taken from the data of Palik[51] (wavelength range 0–2 μm), while for Au it is taken from Johnson and Christy.[52] For our application, we mainly consider the reflection spectra of each array. To measure the reflected spectra from the arrays, a 2D z-normal (in the x–y plane) frequency-domain power monitor is placed at a distance of 500 nm above the array. The colors shown in the figures are obtained by converting the reflection spectra into the International Commission on Illumination (CIE) chromaticity diagram. A unit cell of one dimer was used. The boundary conditions in the x and y directions are periodic to simulate an infinite array of nanosphere dimers. Perfectly matched layer boundary conditions were used in the z-direction to eliminate scattered waves at the boundaries of the simulation region. A mesh override region of a size of 1 nm in all three directions is used around the dimer. For the scattering and absorption cross-sections of the dimer alone, we use a total-field/scattered-field (TFSF) plane-wave source around the dimer together with two power monitor boxes, one in the scattered field region and the other in the total field region. A mesh override region of 1 nm is used around the dimer throughout the TFSF source region. For the oblique angle of incidence plots in Figure 5, the broadband fixed-angle source technique (BFAST) is used, and the mesh override region around the dimer is set to 2 nm. To find the polarization of the reflected light, a polar ellipse analysis object is placed at a distance of 510 nm above the array.

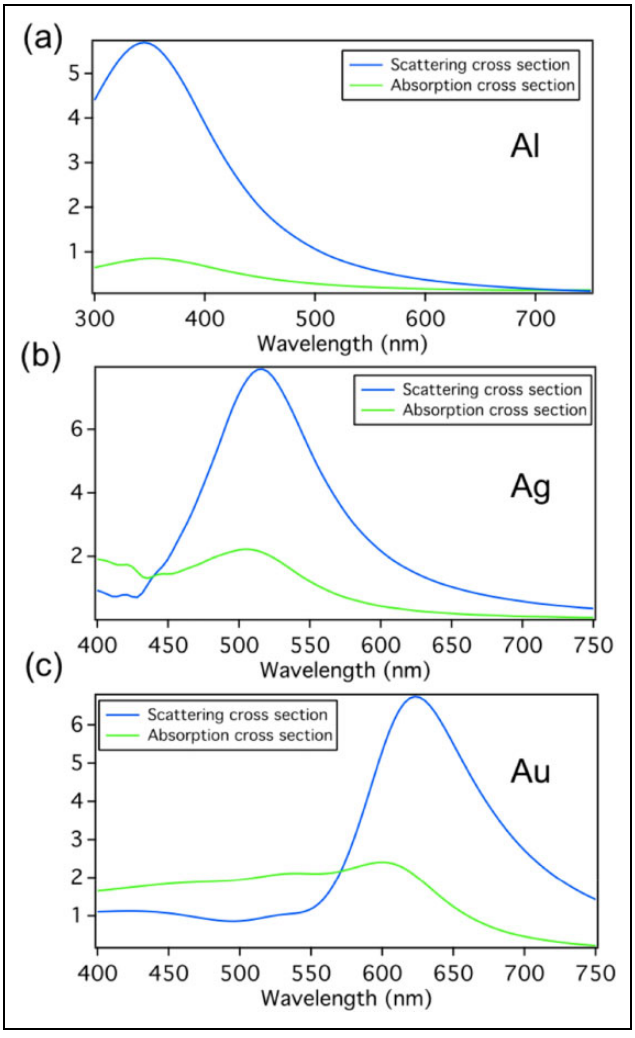

Figure 2. Scattering and absorption cross-sections for the dimer alone without the array for the (a) Al dimer with a sphere radius of 35 nm. A scattering peak is observed at a wavelength of 341 nm. (b) Ag dimer with a sphere radius of 40 nm. The scattering peak wavelength is at 513 nm. (c) Au dimer with a sphere radius of 50 nm, where the scattering peak wavelength is at 619.2 nm. The gap size is 3 nm in all of the dimers. Al: aluminum; Ag: silver; Au: gold.

Results and analysis

Figure 2(a) to (c) shows the scattering and absorption cross-sections of the dimer alone without the array for the Al (radius 35 nm), Ag (radius 40 nm), and Au (radius 50 nm) dimers used for the blue, green, and red pixels, respectively. The gap size in all the dimers is 3 nm. The results show that at resonance, the scattering is significantly higher than the absorption for the three dimers, which is good for this application. The scattering peak is at the wavelength of 341 nm, 513 nm, and 619 nm for each of the Al, Ag, and Au dimers, respectively. Placing the dimer in an array will further shift, enhance, and narrow the resonance peak, as is shown below. Figure 3 shows the reflection spectra of dimer arrays on a glass substrate for the three configurations used for blue, green, and red obtained under p-polarized light at normal

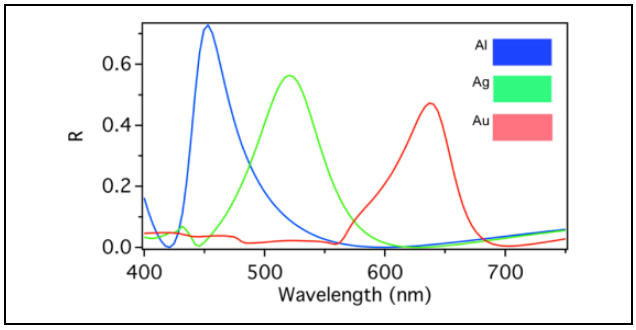

Figure 3. The reflection spectra of dimer arrays on a glass substrate for the three configurations used for blue, green, and red, respectively, obtained under p-polarized light at normal incidence with a wavelength ranging from 400 nm to 750 nm. The spectral peak positions correspond to the wavelengths of blue (453 nm), green (520 nm), and red (637 nm).

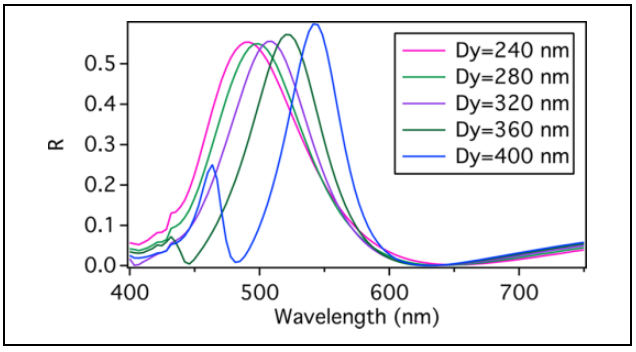

Figure 5. Shows the reflection spectra of the array used for the green pixel where D_y is varied from 240 nm to 400 nm in steps of 40 nm, while D_x is kept fixed at 240 nm. As D_y increases, the collective resonance of the array redshifts and its linewidth narrows which is useful for producing purer colors.

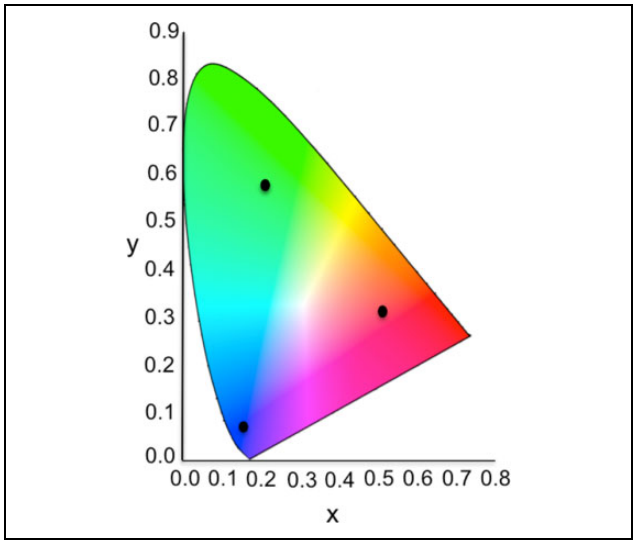

Figure 4. The International Commission on Illumination (CIE) chromaticity diagram coordinates for each color are $X = 13.0485$, $Y = 5.5355$, $Z = 66.9152$, $x = 0.1526$, and $y = 0.0647$ for the blue; $X = 7.4466$, $Y = 19.5526$, $Z = 7.3495$, $x = 0.2167$, and $y = 0.5692$ for the green; and $X = 16.0995$, $Y = 9.3116$, $Z = 3.7168$, $x = 0.5527$, and $y = 0.3196$ for the red.

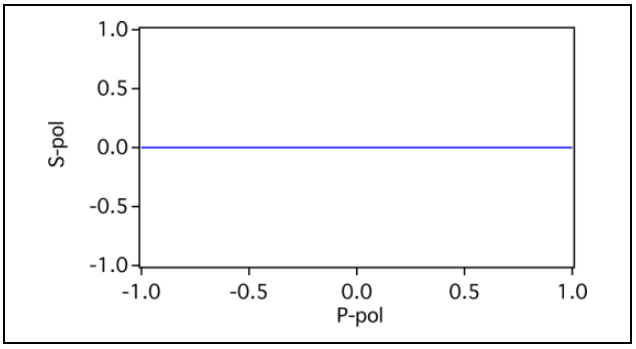

Figure 6. The polarization state of the reflected light. The figure shows that it is p-polarized as expected, since the longitudinal plasmon resonance along the axis of the dimer is the main contributor to the resonance and therefore to the color of the pixel.

incidence with a wavelength ranging from 400 nm to 750 nm. Note that in the case of the red array, the increased radiative damping broadens the resonance; these additional wavelengths modify the perceived color into a pastel red. The CIE chromaticity diagram coordinates for each color are $X = 13.0485$, $Y = 5.5355$, $Z = 66.9152$, $x = 0.1526$, and $y = 0.0647$ for the blue; $X = 7.4466$, $Y = 19.5526$, $Z = 7.3495$, $x = 0.2167$, and $y = 0.5692$ for the green; and $X = 16.0995$, $Y = 9.3116$, $Z = 3.7168$, $x = 0.5527$, and $y = 0.3196$ for the red, as shown in Figure 4.

Figure 5 shows the reflection spectra of the array used for the green pixel, where D_y is varied from 240 nm to 440 nm in steps of 40 nm, while D_x is kept fixed at 240 nm. As D_y increases, the collective resonance of the array is enhanced, redshifted, and narrowed as compared to the isolated Ag dimer in Figure 2(b), which is useful for producing purer colors. Similar results are found for the other arrays. This result is in agreement with the sharpening and narrowing of the array resonance as the period is approaching the diffraction edge as was shown in the study by Zou and Schatz.[34]

Figure 6 shows the polarization state of the reflected light for the array used in the green pixel. Similar results are found for the other arrays. The reflected light is p-polarized as expected, because the longitudinal plasmon resonance along the axis of the dimer is the main contributor to resonance and, therefore, to the color of the pixel. Finally, we show that it is possible to obtain different colors by varying the angle of incidence. Figure 7(a) to (c) shows the reflection spectrum for each array as the angle of incidence is changed from 0° to 60° and the corresponding color for each angle. In addition, we show in the Online supplementary material how the far-field scattering cross-section increases as the gap size is decreased, and the different colors obtained when changing each of the periodicities in y (D_y), the size of the dimer, or the substrate thickness.

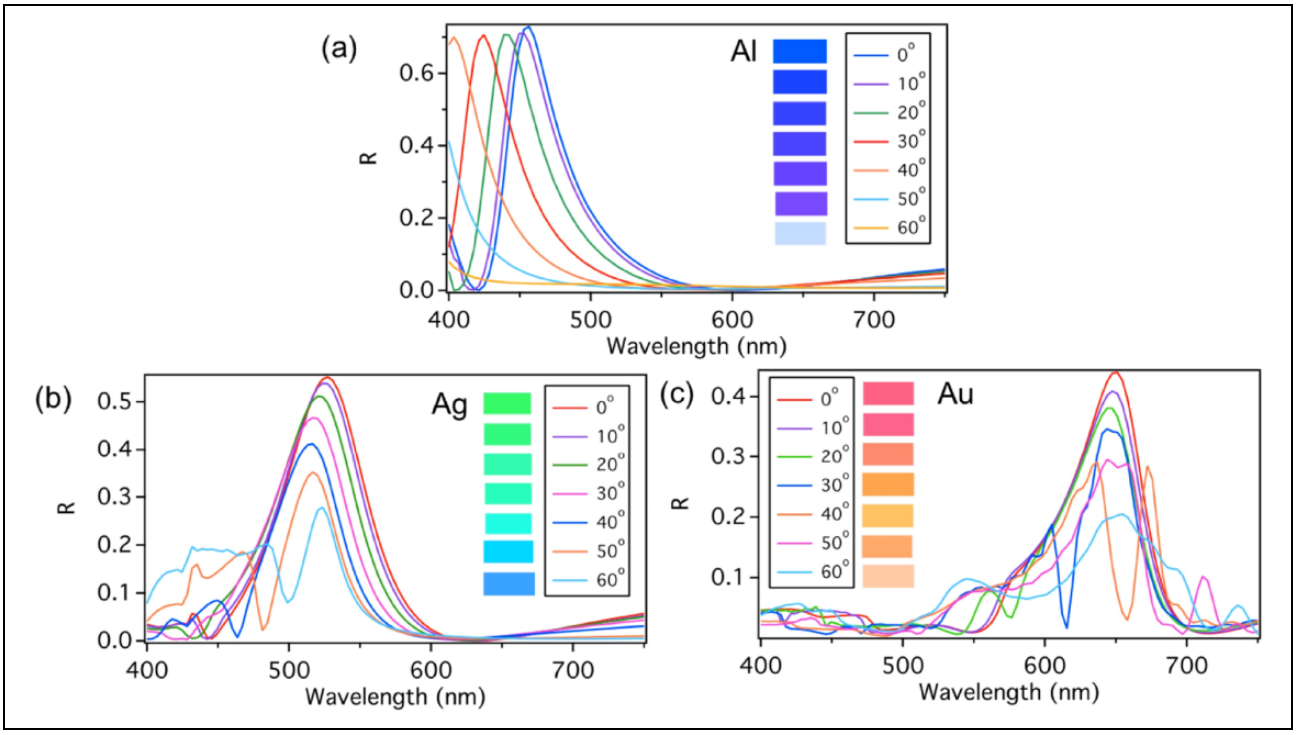

Figure 7. The reflection spectrum for each of the arrays of the (a) blue, (b) green, and (c) red pixels as the angle of incidence is changed from 0° too 60°, and the corresponding color for each angle.

Conclusion

We have demonstrated numerically that highly polarized bright plasmonic color pixels enabled by the selective scattering of Al, Ag, and Au nanosphere dimers arranged in periodic arrays on a glass substrate. We showed that it is possible to obtain RGB pixels in the reflection mode. Far-field diffraction coupling further shifts and enhances the scattering intensity, narrowing the plasmon linewidth for brighter and more vivid colors. The longitudinal plasmon resonance along the axis of the dimer is the main contributor to resonance, and the colors are tuned using a combination of the dimer length and the inter-dimer spacing in the array D_x and D_y. We further showed that it is possible to obtain different colors by varying the angle of incidence. The advantages of this approach include simplicity of the design, bright coloration, and highly polarized function. Our design can also be used for transparent displays by projecting monochromatic light at the resonant wavelength.

Acknowledgment

The authors thank Structural Molecular Imaging Light Enhanced spectroscopies (SMILEs) lab members for the fruitful discussions and suggestions.

Declaration of conflicting interests

The author(s) declared no potential conflicts of interest with respect to the research, authorship, and/or publication of this article.

Funding

The author(s) disclosed receipt of the following financial support for the research, authorship, and/or publication of this article: This study was financially supported by the King Abdullah University of Science and Technology start-up funding.

Supplemental material

Supplementary material for this article is available online.

References

1. Hayashi S and Okamoto T. Plasmonics: visit the past to know the future. *J Phys D Appl Phys* 2012; 45(43): 433001.
2. Maier SA. *Plasmonics: fundamentals and applications*. United Kingdom: Springer, 2007.
3. Kelly K, Coronado E, Zhao L, et al. The optical properties of metal nanoparticles: the influence of size, shape, and dielectric environment. *J Phys Chem* 2003; 107(3): 668–677.
4. Enoch S and Bonod N. *Plasmonics: from basics to advanced topics*. New York: Springer, 2012.
5. Gu Y, Zhang L, Yang J, et al. Color generation via subwavelength plasmonic nanostructures. *Nanoscale* 2015; 7: 6409–6419.
6. Zeng B, Gao Y and Bartoli F. Ultrathin nanostructured metals for highly transmissive plasmonic subtractive color filters. *Sci Rep* 2013; 3: 2840.
7. Yang C, Shen W, Zhang Y, et al. Design and simulation of omnidirectional reflective color filters based on metal-dielectric-metal structure. *Opt Exp* 2014; 22 (9): 11384.

8. Zaccaria R, Francesco Bisio Das G, et al. Plasmonic color-graded nanosystems with achromatic subwavelength architectures for light filtering and advanced SERS detection. *ACS Appl Mater Interfaces* 2016; 8: 8024–8031.
9. Hu X, Sun L, Zeng B, et al. Polarization-independent plasmonic subtractive color filtering in ultrathin Ag nanodisks with high transmission. *Appl Opt* 2016; 55(1): 148–152.
10. Hedayati M and Elbahri M. Review of metasurface plasmonic structural color. *Plasmonics* 2016; 12(5): 1–17.
11. Xu T, Wu Y, Luo X, et al. Plasmonic nanoresonators for high-resolution colour filtering and spectral imaging. *Nature Commun* 2010; 1: 59.
12. Ye M, Sun L, Hu X, et al. Angle-insensitive plasmonic color filters with randomly distributed silver nanodisks. *Opt Lett* 2015; 40(21): 4979–4982.
13. Kristensen A, Yang J, Bozhevolnyi S, et al. Plasmonic colour generation. *Nature Rev Mater* 2016; 2: 16088.
14. Chen Q and Cumming D. High transmission and low color cross-talk plasmonic color filters using triangular-lattice hole arrays in aluminum films. *Opt Exp* 2010; 18(13): 14056.
15. Lee S and Ju B. Wide-gamut plasmonic color filters using a complementary design method. *Sci Rep* 2017; 7: 40649.
16. Olson J, Manjavacas A, Liu L, et al. Vivid, full-color aluminum plasmonic pixels. *PNAS* 2014; 111(40): 14348–14353.
17. Fan J and Wu W. Metal-dielectric-metal plasmonic nanohelms as broad-color-gamut tunable pixels for vivid display. In: *Micro Electro Mechanical Systems (MEMS), IEEE 29th International Conference*, Shanghai, China, 24–28 January 2016. New York: IEEE.
18. Chen T and Reinhard B. Assembling color on the nanoscale: multichromatic switchable pixels from plasmonic atoms and molecules. *Adv Mater* 2016; 28(18): 3522–3527.
19. Fan J, Li Z, Chen Z, et al. Standing-wave resonances in plasmonic nanoumbrella cavities for color generation and colorimetric refractive index sensor. *Appl Surf Sci* 2016; 384: 534–538.
20. Wang G, Chen X, Liu S, et al. Mechanical chameleon through dynamic real-time plasmonic *tuning*. *ACS Nano* 2016; 10(2): 1788–1794.
21. Fan J, Wu W, Chen Z, et al. Three-dimensional cavity nanoantennas with resonant-enhanced surface plasmons as dynamic color-tuning reflectors. *Nanoscale* 2017; 9: 3416–3423.
22. Franklin D, Chen Y, Vazquez-Guardado A, et al. Polarization-independent actively tunable colour generation on imprinted plasmonic surfaces. *Nature Commun* 2015; 6: 7337.
23. Goh X, Zheng Y, Tan S, et al. Three-dimensional plasmonic stereoscopic prints in full colour. *Nature Commun* 2014; 5: 5361.
24. Roberts A, Pors A, Albrektsen O, et al. Subwavelength plasmonic color printing protected for ambient use. *Nano Lett* 2014; 14(2): 783–787.
25. Cheng F, Gao J, Luk T, et al. Structural color printing based on plasmonic metasurfaces of perfect light absorption. *Sci Rep* 2015; 5: 11045.
26. Kumar K, Duan H, Ravi Hegde S, et al. Printing colour at the optical diffraction limit. *Nature Nanotechnol* 2012; 7: 557–561.
27. Wei Hsu C, Zhen B, Qiu W, et al. Transparent displays enabled by resonant nanoparticle scattering. *Nature Commun* 2014; 5: 3152.
28. Huang Y, Chen W, Tsai W, et al. Aluminum plasmonic multicolor meta-hologram. *Nano Lett* 2015; 15(5): 3122–3127.
29. Wang B, Dong F, Li Q, et al. Visible-frequency dielectric metasurfaces for multiwavelength achromatic and highly dispersive holograms. *Nano Lett* 2016; 16(8): 5235–5240.
30. Montelongo Y, Tenorio-Pearl J, Williams C, et al. Plasmonic nanoparticle scattering for color holograms. *PNAS* 2014; 111(35): 12679–12683.
31. Hicks E, Zou S, Schatz G, et al. Controlling plasmon line shapes through diffractive coupling in linear arrays of cylindrical nanoparticles fabricated by electron beam lithography. *Nano Lett* 2005; 5(6): 1065–1070.
32. Zou S, Janel N and Schatz G. Silver nanoparticle array structures that produce remarkably narrow plasmon line shapes. *J Chem Phys* 2004; 120: 10871.
33. Kravets V, Schedin F and Grigorenko A. Extremely narrow plasmon resonances based on diffraction coupling of localized plasmons in arrays of metallic nanoparticles. *Phys Rev Lett* 2008; 101: 087403.
34. Zou S and Schatz G. Generating narrow plasmon resonances from silver nanoparticle arrays: influence of array pattern and particle spacing. In: *Optical Science and Technology, the SPIE 49th Annual Meeting* 2004; Denver, Colorado, United States. Proc. SPIE 5513, Physical Chemistry of Interfaces and Nanomaterials III. doi: 10.1117/12.556064.
35. McLellan E, Gunnarsson L, Rindzevicius T, et al. Plasmonic and diffractive coupling in 2D arrays of nanoparticles produced by electron beam lithography. *Mater Res Soc Symp Proc* 2007; 951.
36. Lamprecht B, Schider G, Lechner RT, et al. Metal nanoparticle gratings: influence of dipolar particle interaction on the plasmon resonance. *Phys Rev Lett* 2000; 84(20): 4721–4724.
37. Zou S and Schatz G. Narrow plasmonic/photonic extinction and scattering line shapes for one and two dimensional silver nanoparticle arrays. *J Chem Phys* 2004; 121(24): 12606–12612.
38. Auguie B and Barnes W. Collective resonances in gold nanoparticle arrays. *Phys Rev Lett* 2008; 101: 143902.
39. Malinsky M, Kelly K, Schatz G, et al. Nanosphere lithography: effect of substrate on the localized surface plasmon resonance. *J Phys Chem B* 2001; 105: 2343–2350.
40. Pinchuk A, Hilger A, Plessen G, et al. Substrate effect on the optical response of silver nanoparticles. *Nanotechnology* 2004; 15(12).
41. Knight M, Wu Y, Lassiter J, et al. Substrates matter: influence of an adjacent dielectric on an individual plasmonic nanoparticle. *Nano Lett* 2009; 9(5): 2188–2192.
42. Wu Y and Nordlander P. Finite-Difference Time-Domain Modeling of the Optical Properties of Nanoparticles near Dielectric Substrates. *J Phys Chem C* 2010; 114(16): 7302–7307.

43. Felidj N, Laurent G, Aubard J, et al. Grating-induced plasmon mode in gold nanoparticle arrays. *J Chem Phys* 2005; 123: 22 1103.
44. Adato R, Yanik AA, Amsden JJ, et al. Ultra-sensitive vibrational spectroscopy of protein monolayers with plasmonic nanoantenna arrays. *Proc Natl Acad Sci USA* 2009; 106(46): 19227–19232.
45. Qin F, Cui X, Ruan Q, et al. Role of shape in substrate-induced plasmonic shift and mode uncovering on gold nanocrystals. *Nanoscale* 2016; 8: 17645–17657.
46. Sikdar D, Zhu W, Cheng W, et al. Substrate-mediated broadband tunability in plasmonic resonances of metal nanoantennas on finite high-permittivity dielectric substrate. *Plasmonics* 2015; 10(6): 1663–1673.
47. Zhang S, Bao K, Halas N, et al. Substrate-induced Fano resonances of a plasmonic nanocube: a route to increased-sensitivity localized surface plasmon resonance sensors revealed. *Nano Lett* 2011; 11(4): 1657–1663.
48. Huang Y, Zhou Q, Hou M, et al. Nanogap effects on near- and far-field plasmonic behaviors of metallic nanoparticle dimers. *Phys Chem Chem Phys* 2015; 17: 29293.
49. Gargiulo J, Brick T, Violi I, et al. Understanding and reducing photothermal forces for the fabrication of Au nanoparticle dimers by optical printing. *Nano Lett* 2017; 17: 5747−5755.
50. Flauraud V, Mastrangeli M, Bernasconi G, et al. Nanoscale topographical control of capillary assembly of nanoparticles. *Nature Nanotechnol* 2017; 12: 73–80.
51. Palik ED. *Handbook of optical constants of solids*. Amsterdam: Academic Press, 1985.
52. Johnson P and Christy R. Optical constants of the noble metals. *Phys Rev B* 1972; 6(12): 4370–4379.